International Journal of Emerging Technology and Advanced Engineering
Website: www.ijetae.com (ISSN 2250-2459, ISO 9001:2008 Certified Journal, Volume 5, Issue 1, January 2015)

Integer Implementation of 3D Wavelet Transform for Lossy Data Compression

Teerapong Orachon[1], Suvit Poomrittigul[2], Taichi Yoshida[3], Masahiro Iwahashi[4], Somchart Chokchaitam[5]
[1,3,4]*Department of Electrical Engineering, Nagaoka University of Technology, Nagaoka, Japan*
[2]*Department of Computer Technology, Pathumwan Institute of Technology, Bangkok, Thailand*
[5]*Department of Electrical Engineering, Thammasat University, Bangkok, Thailand*

***Abstract*— A new non-separable 2D structure is proposed for integer implementation of a 3D lifting wavelet transform. It reduces total amount of rounding noise due to expressing signal values as integers inside the transform. In the existing method, a non-separable 3D structure is used to minimize lifting steps. It contributes to decrease delay from input to output. As it decreases total number of rounding operations which are source of the rounding error, total amount of the rounding noise was also reduced in the (5,3) type transform for lossless coding. However, it was found that it is not true in the (9,7) type transform for lossy coding. In this paper, introducing a non-separable 2D structure instead of the 3D structure, a new transform with reduced number of lifting steps is proposed. Since the proposed method does not change order of the original lifting steps, total amount of the rounding noise observed in pixel values of the decoded image is significantly reduced. Upper bound of quality of decoded images in lossy coding is also improved.**

***Keywords*—coding, compression, image, JPEG, wavelet.**

I. Introduction

Owing to internationalization of data compression algorithm such as JPEG and MPEG, digital image and video have been shared via worldwide internet. It has been contributing marvellous development of various types of digital multimedia technologies from one-dimensional (1D) audio signals and two-dimensional (2D) image signals to three-dimensional (3D) signals. So far, various types of 3D wavelet transforms have been reported for analysis on video signals [1], hyperspectral images [2], integral images [3] and medical volumetric data [4]. Implementation issues such as processing speed, memory space [5], LSI architecture [6] are also important for product development in consumer electronics. This paper deals with integer implementation of 3D wavelet transform for lossy data compression of 3D signals.

Ever since JPEG 2000 international standard adopted the wavelet transform [7, 8], and it was applied to data compression of digital cinema video signals [9,10], wavelet transforms have been attracting researchers' attention.

Most of previously reported transforms have been converged to two representative types. One is the (5,3) type transform for lossless coding of images. Another is the (9,7) type transform for lossy coding. The former is based on double lifting steps. Since signal values are rounded into integers inside the transform, transformed signals are also expressed as integers. Furthermore, those rounding noises are perfectly cancelled at output of the backward transform. This property makes it possible to decode the original integer input signal without any loss. Therefore the (5,3) type transform has been used for lossless coding of images. Introducing quantization between the forward transform and entropy coding, it also becomes possible to perform lossy coding. However its performance is inferior to the (9,7) type transform in lossy coding mode.

Since this paper focuses on lossy coding of 3D signals, the (9,7) type transform based on quadruple lifting steps is analysed. In its implementation, there are two aspects dealt with in this paper. One is delay from input to output. As a lifting step must wait for calculation result of its previous lifting step, many sequential lifting steps brings about long delay from input to output. Another aspect is integer implementation of the transform. Ideally, signal values inside the transform are assume to be real numbers. However, in practice, those are rounded into finite word length rational numbers. Shorter word length means lower computational load, but more rounding noise. It contributes to reducing memory space in trade off with the rounding noise [11]. Note that the rounding noise is independent of coding efficiency, whereas the quantization noise is closely related to performance in lossy coding.

To overcome the delay problem, a non-separable 2D structure was introduced to (5,3) type 2D transform [12,13]. It was extended to be adaptive to local property of pixels to increase precision of the prediction [14-16]. It contributed to reducing total amount of the rounding noise in integer implementation of the (5,3) type 2D transform. It was also true for 3D case [17]. However it is not always true for the (9, 7) type transform.

International Journal of Emerging Technology and Advanced Engineering
Website: www.ijetae.com (ISSN 2250-2459, ISO 9001:2008 Certified Journal, Volume 5, Issue 1, January 2015)

Even though introduction of non-separable structures surely reduces total number of lifting steps [18-21], total amount of the rounding noise was not always reduced [22, 23]. This problem still remains in 3D case (existing method) [24].

In this paper, non-separable 2D structures are introduced instead of the 3D structure in the existing method. Unlike the existing method, order of the lifting steps in the original separable 3D transform is preserved. As a result, total amount of the rounding noise is reduced, even though total number of the rounding operations is increased comparing to the existing method. It is experimentally confirmed that total amount of the rounding noise observed in pixel values of the decoded image is significantly reduced. Upper bound of quality of decoded images in lossy coding mode is also improved.

This paper is organized as follows. The (9, 7) type 3D wavelet transform and its problem in integer implementation is addressed in II. The existing method composed of non-separable 3D structure is summarized in III. Non-separable 2D structure is newly introduced for the 3D wavelet transform in IV. The proposed method is compared to the existing method in respect of the rounding noise and lossy coding performance in V. This paper is concluded in VI.

II. Problem Setting

Focus of this paper is addressed. Problem to be tackled in this paper is summarized.

A. Two Types of Wavelet Transform

Fig. 1(a) illustrates a forward transform of (5, 3) type wavelet transform developed for 'lossless' coding of 1D signals in JPEG 2000 [7]. It is composed of two lifting steps. Fig. 1 (b) illustrates a (9, 7) type transform developed for 'lossy' coding. Two more lifting steps and scaling with a constant k are added. This paper focuses on the (9, 7) type transform for 'lossy' coding of 3D signals. Especially, a problem related to integer implementation of the transform is addressed.

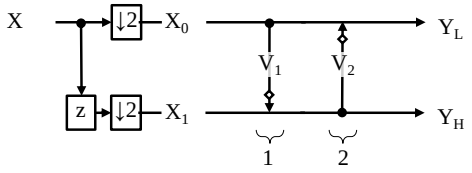

(a) (5,3) type for lossless coding.

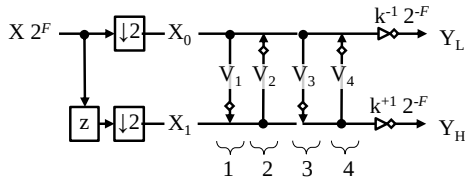

(b) (9,7) type for lossy coding

Fig.1 Two types of wavelet transform.

In detail, the (5,3) type transform decomposes a 1D input signal X into two frequency band signals Y_L and Y_H with two lifting steps. Firstly, the input signal $x(n)$, n= 0, 1, ⋯, N-1 is divided into two groups $x_0(m)$ and $x_1(m)$, m= 0, 1, ⋯, M -1, M=N/2. It is expressed with the z transform as

$$X_c(z) = \downarrow 2[z^c X(z)], \quad c \in \{0,1\} \tag{1}$$

for

$$\downarrow 2[X(z)] = \frac{1}{Q}\sum_{p=0}^{Q-1} X(z^{1/Q} \cdot W_Q^p), \quad W_Q = e^{j2\pi/Q} \tag{2}$$

where Q=2 and

$$X(z) = \sum_{n=0}^{N-1} x(n) z^{-n}. \tag{3}$$

Secondly, the 1st lifting step is applied as

$$X_1^{(1)}(z) = X_1(z) + R[V_1(z) X_0(z)] \tag{4}$$

And the 2nd lifting is applied as

$$X_0^{(2)}(z) = X_0(z) + R[V_2(z) X_1^{(1)}(z)] \tag{5}$$

Where $V_1(z)$ and $V_2(z)$ are filters given as

$$\begin{bmatrix} V_1(z) \\ V_2(z) \end{bmatrix} = \begin{bmatrix} \alpha \cdot (1 + z^{+1}) \\ \beta \cdot (1 + z^{-1}) \end{bmatrix} \tag{6}$$

For (α, β)=(-1/2, 1/4) in the (5,3) type transform in JPEG 2000. Finally the frequency band signals are generated as

$$\begin{bmatrix} Y_L(z) \\ Y_H(z) \end{bmatrix} = \begin{bmatrix} X_0^{(2)} \\ X_1^{(1)} \end{bmatrix} \tag{7}$$

for

$$Y_b(z) = \sum_{m=0}^{M-1} y_b(m) z^{-m}, \quad b \in \{L, H\}. \tag{8}$$

International Journal of Emerging Technology and Advanced Engineering
Website: www.ijetae.com (ISSN 2250-2459, ISO 9001:2008 Certified Journal, Volume 5, Issue 1, January 2015)

Note that $R[\ ]$ in (4) and (5) is the rounding operator which truncates a pixel value in real number to an integer. This is the source of the rounding noise to be reduced in this paper.

B. Integer Implementation of the Transform

The (9, 7) type transform has two more lifting steps and scaling. Namely, the 3rd lifting step

$$X_1^{(3)}(z) = X_1^{(1)}(z) + R[V_3(z)X_0^{(2)}(z)] \tag{9}$$

and the 4-th lifting step

$$X_0^{(4)}(z) = X_0^{(2)}(z) + R[V_4(z)X_1^{(3)}(z)] \tag{10}$$

are added where $V_3(z)$ and $V_4(z)$ are given as

$$\begin{bmatrix} V_3(z) \\ V_4(z) \end{bmatrix} = \begin{bmatrix} \gamma \cdot (1+z^{+1}) \\ \delta \cdot (1+z^{-1}) \end{bmatrix} \tag{11}$$

Where

$$\begin{cases} \alpha = -1.586134342059924, \\ \beta = -0.052980118572961, \\ \gamma = 0.882911075530934, \\ \delta = 0.443506852043971, \\ k = 1.230174104914001 \end{cases} \tag{12}$$

in the (9,7) type transform in JPEG 2000. Finally the frequency band signals are generated with scaling as

$$\begin{bmatrix} Y_L(z) \\ Y_H(z) \end{bmatrix} = \begin{bmatrix} R[k^{-1}2^{-F}X_0^{(4)}] \\ R[k^{+1}2^{-F}X_1^{(3)}] \end{bmatrix}. \tag{13}$$

Note that the input signal is scaled with 2^F beforehand as illustrated in Fig. 1(b).

In the integer implementation, F is set to a positive number. The smaller the F is, the shorter the bit depth of signals inside the transform becomes. It contributes to reduce hardware complexity for implementation of the transform in general.

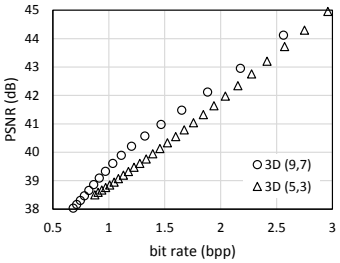

Fig.2 Lossy coding performance.

Fig. 2 compares the (5, 3) type 3D transform in [17] and the (9, 7) type 3D transform (F=8) in [24] in respect of 'lossy' coding performance. The horizontal axis denotes the bit rate (= code length per pixel). The frequency band signals are quantized with the optimum bit allocation, and entropy coded according to JPEG 2000. The lower the bit rate is, the better the data compression ratio becomes. The vertical axis denotes the peak-signal to noise ratio (PSNR). Larger value means higher quality of the decoded image. As it is well known, it is confirmed that the (9,7) type is better than the (5,3) type in 'lossy' coding of a 3D signal. Therefore this paper focuses on improving the (9, 7) type transform for lossy compression of 3D signals.

C. Problem in Integer Implementation

Fig. 3(a) compares two structures for the (9,7) type 3D wavelet transform at F=3. One is the separable 3D structure (Sep) in which the 1D transform in Fig. 1(b) is applied three times. Namely, in horizontal direction, in vertical direction, and in inter-frames. Another one is the non-separable 3D structure (Ns3D) reported in [24]. It has advantage that it is composed of the minimum number of lifting steps. However it has a problem described as below.

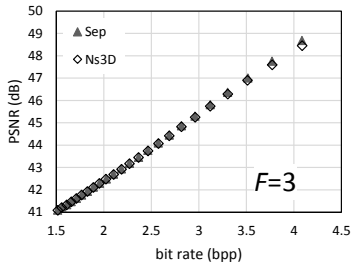

(a) F=3

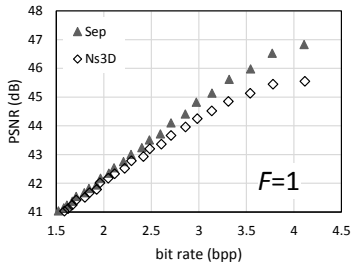

(b) F=1

Fig.3 Image quality degradation in integer implementation of the (9,7) type wavelet transform.

Fig. 3(b) compares the two structures at F=1. In this case, hardware complexity is reduced as F is set to shorter value. However, as observed in the figure, PSNR is lowered.

International Journal of Emerging Technology and Advanced Engineering
Website: www.ijetae.com (ISSN 2250-2459, ISO 9001:2008 Certified Journal, Volume 5, Issue 1, January 2015)

It means that quality of the decoded image is degraded by the rounding noise. In detail, the quantization noise generated in the lossy encoder after the forward transform contributes to increase the compression ratio. On the contrary, the rounding noise generated by the rounding operator does not increase the ratio. It determines the upper bound of PSNR in the rate distortion curve as illustrated in Fig.3. This paper aims at increasing the PSNR bound of the existing Ns3D.

III. Existing Method

The existing method of the 3D wavelet transform is detailed. The number of lifting steps is decreased using non-separable structures.

A. Separable 3D Structure (Sep)

Fig. 4 illustrates the (9, 7) type separable 3D wavelet transform (Sep). As a result of applying the 1D structure three times, it has 12 lifting steps. It becomes demerit for fast implementation of the transform because a lifting step must wait for a calculation result of its previous lifting step. It means that the more the lifting steps exist, the longer the delay becomes. To cope with this problem, the minimum lifting wavelet transform was reported in [24] as explained in the next subsection.

Signal processing of Sep is detailed as below. Denoting a 3D input signal as

$$X(z_1,z_2,z_3)=\sum_{n_3=0}^{N_3-1}\sum_{n_2=0}^{N_2-1}\sum_{n_1=0}^{N_1-1}x(n_1,n_2,n_3)z_1^{-n_1}z_2^{-n_2}z_3^{-n_3} \quad (14)$$

the input signal is classified into 8 groups as

$$\begin{cases} X_{c_1c_2c_3}(z_1,z_2,z_3)= \\ \downarrow 2_3[\downarrow 2_2[\downarrow 2_1[z_3^{c_3}z_2^{c_2}z_1^{c_1}X(z_1,z_2,z_3)\cdot 2^F]]], \\ c_1,c_2,c_3\in\{0,1\} \end{cases} \quad (15)$$

for

$$\begin{cases} \downarrow 2_1[X(z_1,z_2,z_3)]=\dfrac{1}{Q}\displaystyle\sum_{p=0}^{Q-1}X(z_1^{1/Q}\cdot W_Q^p,z_2,z_3) \\ \downarrow 2_2[X(z_1,z_2,z_3)]=\dfrac{1}{Q}\displaystyle\sum_{p=0}^{Q-1}X(z_1,z_2^{1/Q}\cdot W_Q^p,z_3) \\ \downarrow 2_3[X(z_1,z_2,z_3)]=\dfrac{1}{Q}\displaystyle\sum_{p=0}^{Q-1}X(z_1,z_2,z_3^{1/Q}\cdot W_Q^p) \end{cases} \quad (16)$$

where Q=2. Next, the filters

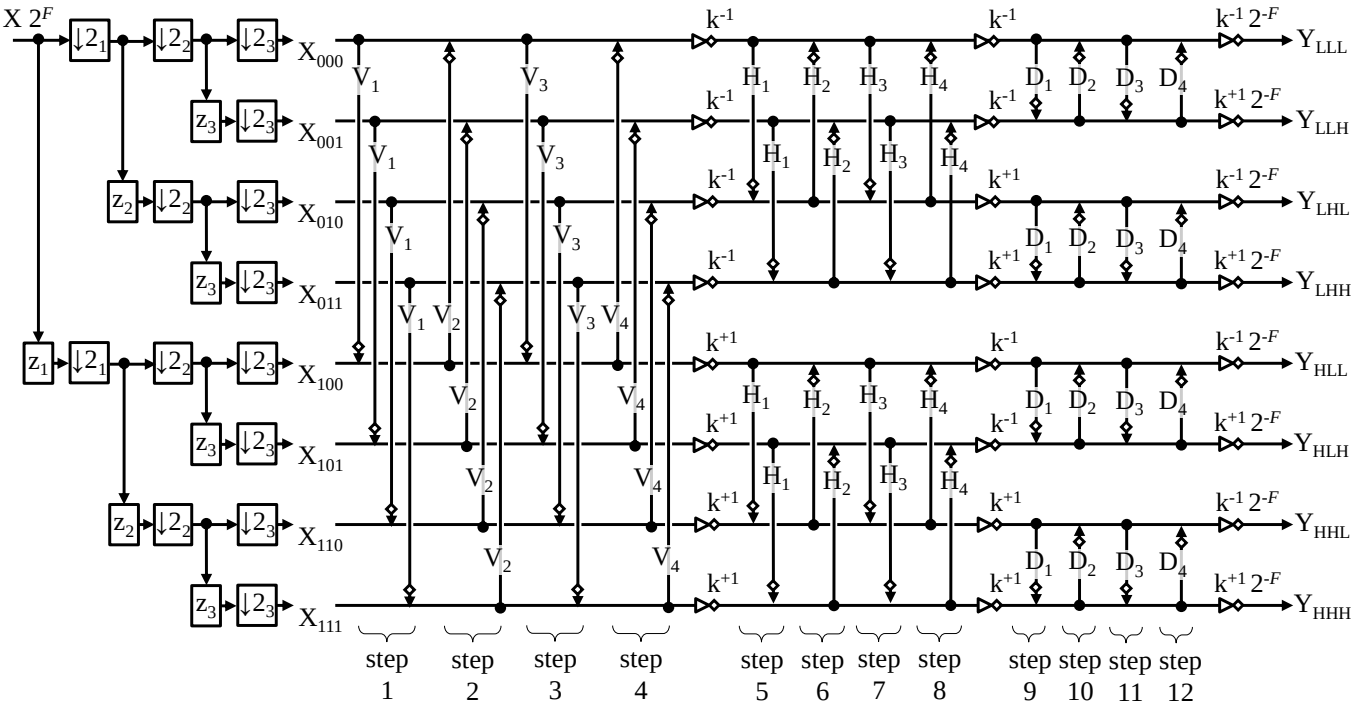

Fig.4 Separable 3D structure 'Sep' for (9,7) type 3D transform.

International Journal of Emerging Technology and Advanced Engineering
Website: www.ijetae.com (ISSN 2250-2459, ISO 9001:2008 Certified Journal, Volume 5, Issue 1, January 2015)

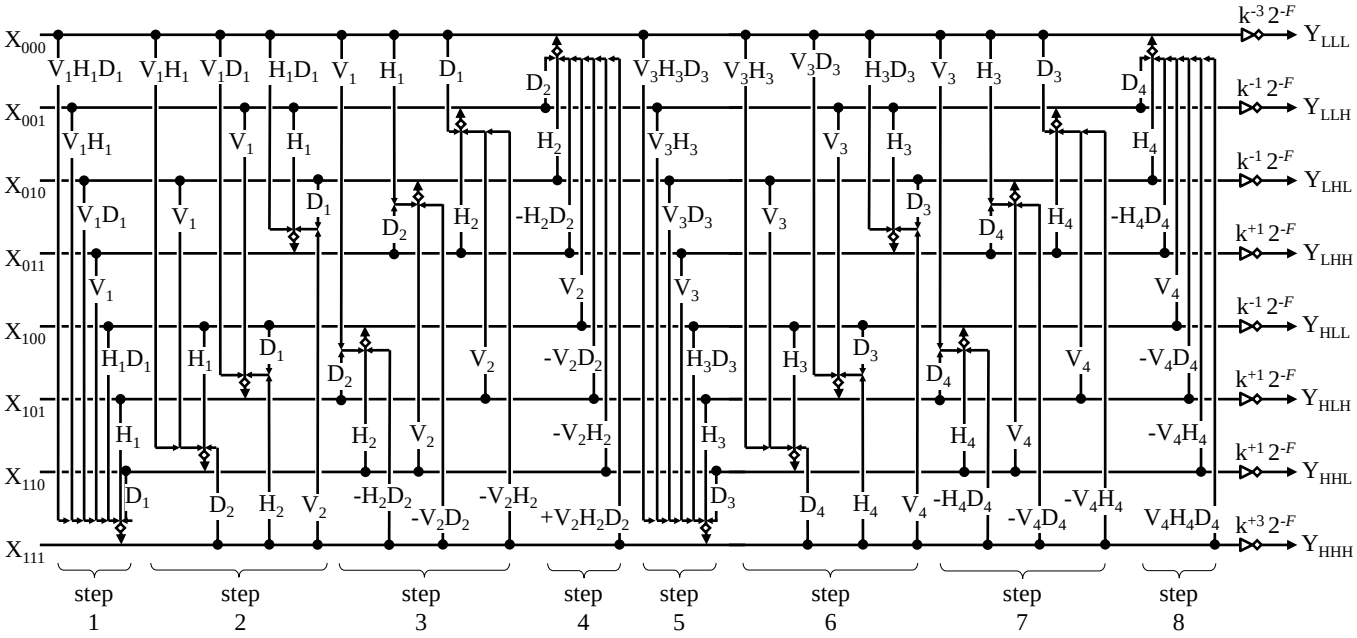

Fig.5 Non-separable 3D structure 'Ns3D' for 3D transform (existing method).

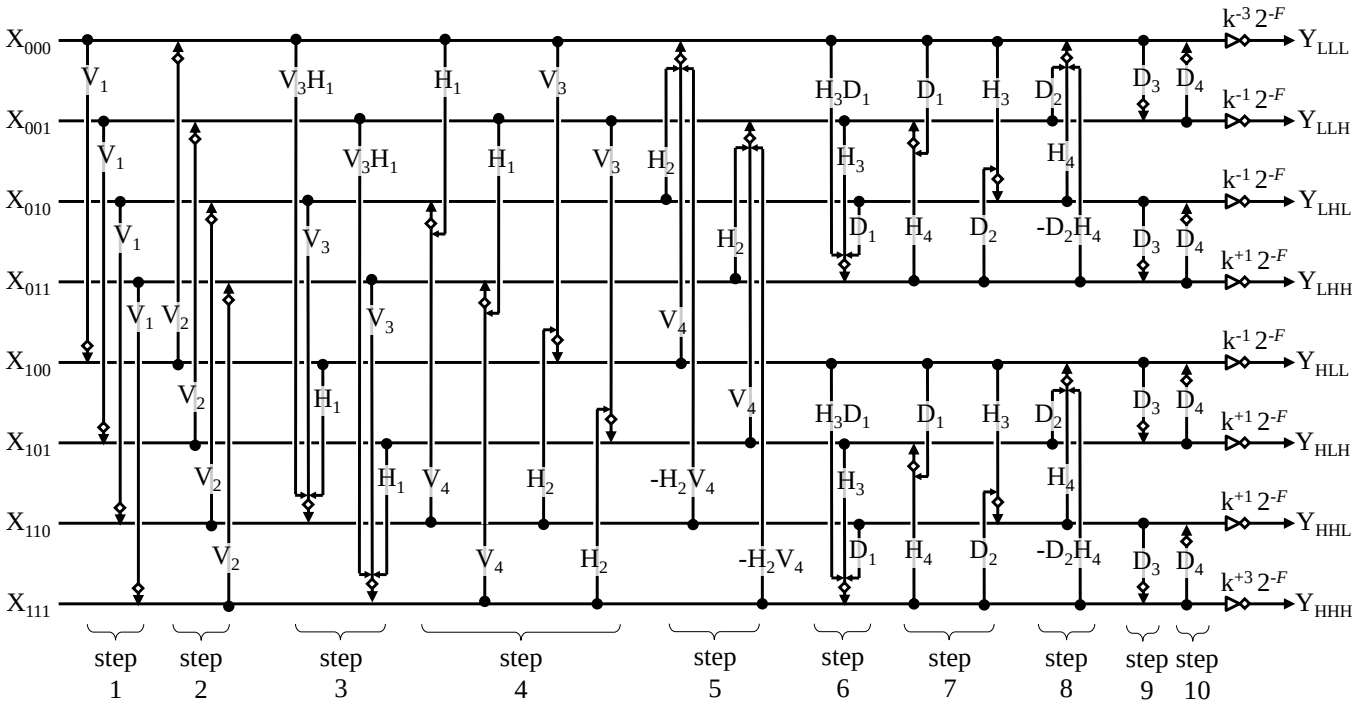

Fig.6 Combination with non-separable 2D structure 'Ns2D' for 3D transform (proposed method).

International Journal of Emerging Technology and Advanced Engineering
Website: www.ijetae.com (ISSN 2250-2459, ISO 9001:2008 Certified Journal, Volume 5, Issue 1, January 2015)

$$\begin{bmatrix} V_1(z_1) & V_3(z_1) \\ V_2(z_1) & V_4(z_1) \end{bmatrix} = \begin{bmatrix} \alpha\cdot(1+z_1^{+1}) & \gamma\cdot(1+z_1^{+1}) \\ \beta\cdot(1+z_1^{-1}) & \delta\cdot(1+z_1^{-1}) \end{bmatrix} \quad (17)$$

$$\begin{bmatrix} H_1(z_2) & H_3(z_2) \\ H_2(z_2) & H_4(z_2) \end{bmatrix} = \begin{bmatrix} \alpha\cdot(1+z_2^{+1}) & \gamma\cdot(1+z_2^{+1}) \\ \beta\cdot(1+z_2^{-1}) & \delta\cdot(1+z_2^{-1}) \end{bmatrix} \quad (18)$$

$$\begin{bmatrix} D_1(z_3) & D_3(z_3) \\ D_2(z_3) & D_4(z_3) \end{bmatrix} = \begin{bmatrix} \alpha\cdot(1+z_3^{+1}) & \gamma\cdot(1+z_3^{+1}) \\ \beta\cdot(1+z_3^{-1}) & \delta\cdot(1+z_3^{-1}) \end{bmatrix} \quad (19)$$

Are applied in the lifting steps. Finally, the 8 frequency band signals are obtained as illustrated in the figure.

B. Non-separable 3D Structure (Ns3D)

Fig. 5 illustrates the existing method (Ns3D) reported in [24]. As illustrated in the figure, it has 8 lifting steps. The total number of lifting steps is decreased from 12 to 8 (66.7 %) comparing to Sep. This is because Ns3D uses non-separable structure in each lifting step. For example, the 1st lifting steps is described as

$$\begin{aligned} X^{(1)}_{111}(\mathbf{z}) &= X_{111}(\mathbf{z}) + R[V_1H_1D_1X_{000}(\mathbf{z}) \\ &+ V_1H_1X_{001}(\mathbf{z}) + V_1D_1X_{010}(\mathbf{z}) + V_1X_{011}(\mathbf{z}) \\ &+ H_1D_1X_{100}(\mathbf{z}) + H_1X_{101}(\mathbf{z}) + D_1X_{110}(\mathbf{z})] \end{aligned} \quad (20)$$

Where $\mathbf{z} = (z_1, z_2, z_3)$. It also requires multi-dimensional memory accessing. For example, $V_1H_1D_1$ and V_1H_1 require 3D and 2D memory accessing, respectively. However, as explained in section **II.***C*, its image quality is degraded in its integer implementation. This problem is eased by the proposed method as explained in the next section.

IV. Proposed Method

The proposed method is summarized as below. Instead of the non-separable 3D structure in the existing method, the non-separable 2D structure is used combining with the separable structure.

A. Non-separable 2D Structure (Ns2D)

Fig. 6 illustrates the proposed method (Ns2D). Unlike the existing method Ns3D, it is composed of non-separable 2D structures in combination with separable structures. As detailed in the next subsection, the number of lifting steps is increased comparing to Ns3D, but not more than Sep. However total amount of the rounding noise is reduced as experimentally confirmed in section **V**.

The 1st and the 2nd lifting steps are 1D structures. Those are expressed as

$$\begin{cases} X^{(1)}_{1c_2c_3}(\mathbf{z}) = X_{1c_2c_3}(\mathbf{z}) + R[V_1X_{0c_2c_3}(\mathbf{z})] \\ X^{(2)}_{0c_2c_3}(\mathbf{z}) = X_{0c_2c_3}(\mathbf{z}) + R[V_1X^{(1)}_{1c_2c_3}(\mathbf{z})] \end{cases} \quad (21)$$

Where c_2, $c_3 \in \{0,1\}$. The 3rd, 4th and 5th lifting steps are non-separable 2D structures. For example, the 1st step is expressed as

$$\begin{aligned} X^{(2)}_{11c_3}(\mathbf{z}) &= X^{(1)}_{11c_3}(\mathbf{z}) + R[V_3V_1X^{(2)}_{00c_3}(\mathbf{z}) \\ &+ V_3X^{(2)}_{01c_3}(\mathbf{z}) + H_1X^{(1)}_{10c_3}(\mathbf{z})] \end{aligned} \quad (22)$$

Where $c_3 \in \{0,1\}$. A set of the 6th, 7th and 8th lifting steps is a non-separable 2D structure. The final set of the 9th and 10th lifting steps is the 1D structure again. Thus, the proposed method is a combination of non-separable 2D structures and a product of 1D structures (= separable structure).

B. Comparison of the Structures

Table I compares three structures: Sep, Ns3D and Ns2D. As summarized in the table, total number of the lifting steps of the proposed Ns2D is increased from 8 to 10 comparing to the existing Ns3D. The total number of the rounding operations is also increased. Note that it is still fewer than Sep. There seems to be no merit in reducing the rounding noise. However the proposed method surely reduces total amount of the rounding noise as confirmed in section **V**. This is considered to be due to the difference between Ns3D and Ns2D described below.

As illustrated in Fig. 4, Sep is composed of the lifting steps V_1, V_2, $\cdots$, D_4 which is expressed as

$$Sep \quad V_1V_2V_3V_4H_1H_2H_3H_4D_1D_2D_3D_4\,. \quad (23)$$

In the existing method, firstly, order of the lifting steps is changed as

$$Sep' \quad V_1V_2H_1H_2D_1D_2V_3V_4H_3H_4D_3D_4\,, \quad (24)$$

And then a part of it is implemented in the non-separable 3D structure as

$$Ns3D \quad [V_1V_2H_1H_2D_1D_2][V_3V_4H_3H_4D_3D_4] \quad (25)$$

Where the [ ] part denotes the non-separable 3D structure. Unlike the existing method in (25), the proposed method expressed as

$$Ns2D \quad V_1V_2(V_3V_4H_1H_2)(H_3H_4D_1D_2)D_3D_4 \quad (26)$$

does not change the order of (23) where the ( ) part denotes the non-separable 2D structure.

International Journal of Emerging Technology and Advanced Engineering
Website: www.ijetae.com (ISSN 2250-2459, ISO 9001:2008 Certified Journal, Volume 5, Issue 1, January 2015)

Table I
Comparison Of The Methods

(9,7) type	Sep	Ns3D	Ns2D
rounding operations	72	24	40
lifting steps	12	8	10
memory accessing	1D	3D	2D

V. EXPERIMENTS

Superiority of the proposed method Ns3D over the existing method Ns2D is experimentally confirmed.

A. Evaluation of Rounding noise

Fig. 7 illustrates a set of MRI volumetric image tested in this paper. It is composed of 8 frames. Each frame is composed of 256×256 pixels. Each pixel has 8 bit depth integer value. Namely, $x(n) \in [0, 255]$. Fig. 8 summarizes result of applying the 3D wavelet transform to the image in Fig. 7.

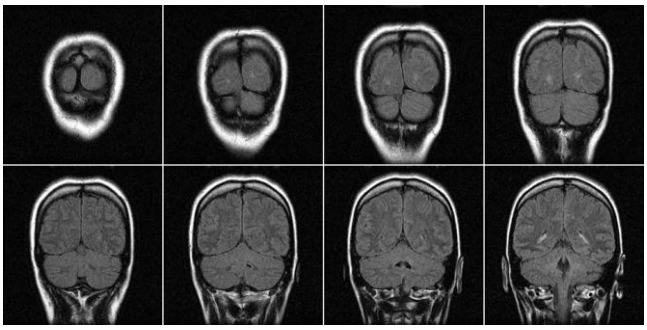

Fig.7 Tested data set 'MRI'.

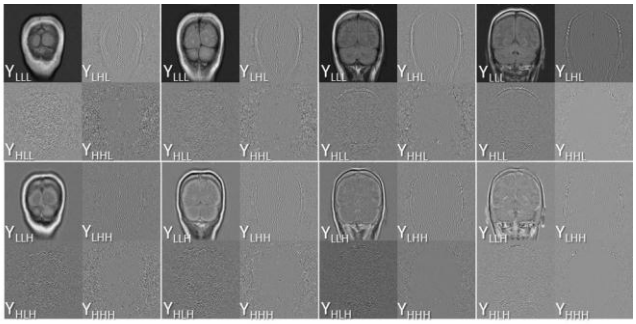

Fig.8 Results of the (9,7) type transform.

B. Evaluation of Rounding Noise

Fig. 9 summarizes variance of the rounding noise observed in each frequency band signals as F=0. In all bands, the existing Ns3D is the biggest (=worst). In contrast, the proposed Ns2D is apparently better than Ns3D.

Variance averaged over all frequency bands are summarized in Fig. 10. An auto-regressive (AR) model and a random signal are added as the input signal. It is clearly observed that the proposed method is the best in respect of variance of the rounding noise in frequency domain.

Fig. 11 summarizes variance of the rounding noise in pixel domain. In the forward transform, no rounding operation is applied. The quantization for lossy coding is not used. In the backward transform, signals are rounded at F=0. Difference between the decoded signal and the input signal is defined as the rounding noise in pixel domain. Its variance is measured with the PSNR defined as

$$PSNR = 20\log_{10} 255 - 10\log_{10} \sigma_{Rnd}^2 \qquad (27)$$

Where σ_{Rnd} denotes the standard deviation of the rounding noise in pixel domain. As confirmed according to the figure, the proposed method significantly reduces total amount of the rounding noise, and has the best quality of the decoded signal.

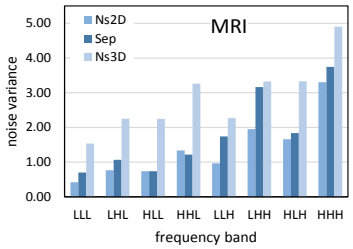

Fig.9 Rounding noise in each frequency band.

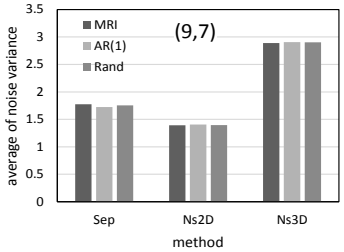

Fig.10 Rounding noise averaged over all frequency bands.

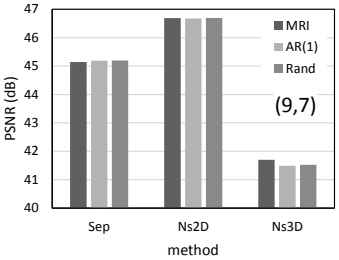

Fig.11 Rounding noise in pixel domain.

International Journal of Emerging Technology and Advanced Engineering
Website: www.ijetae.com (ISSN 2250-2459, ISO 9001:2008 Certified Journal, Volume 5, Issue 1, January 2015)

C. Evaluation of Lossy Coding Performance

Fig. 12 illustrates the rate-distortion curves. It compares performance of the methods in lossy coding mode. In Fig. 12(a) at F=0, the existing Ns3D is the worst at high bit rate. Obviously, the proposed Ns2D is observed to be the best. This PSNR degradation is related to the rounding noise in pixel domain in Fig.11 which determines the upper bound of the PSNR in Fig.12. It can be modelled as

$$PSNR = 20\log_{10} 255 - 10\log_{10}(\sigma_{Rnd}^2 + \sigma_{Qnt}^2) \qquad (28)$$

Where σ_{Rnd} and σ_{Qnt} denotes the standard deviation of the rounding noise and the quantization noise, respectively.

In case of $\sigma_{Qnt} >> \sigma_{Rnd}$ holds, it is well known that the quantization noise is related to the bit rate *Bit* as

$$\frac{\Delta PSNR}{\Delta Bit} = \frac{-10\log_{10}\Delta\sigma_{Qnt}^2}{\Delta Bit} \propto 6.02 \qquad (29)$$

Where Δ denotes deviation of the value. Namely, one bit increase of *Bit* provides 6.02 (dB) increase of the PSNR. It comes from decrease of standard deviation of the quantization noise σ_{Qnt}. In brief, decrease of quantization noise increases PSNR. In contrast, total amount of the rounding noise is independent of PSNR. In case of $\sigma_{Qnt} << \sigma_{Rnd}$ holds, (28) becomes

$$PSNR \approx 20\log_{10} 255 - 10\log_{10}\sigma_{Rnd}^2 \qquad (30)$$

Which determines the upper bound of PSNR in the rate distortion curves.

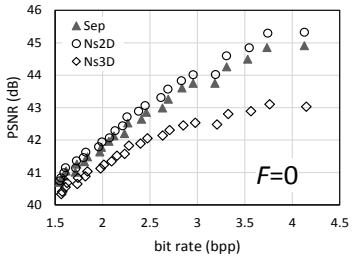

(a) F=0

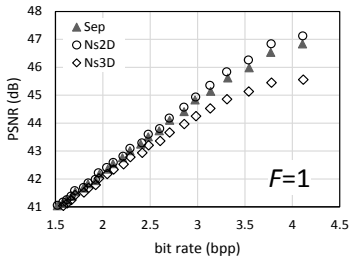

(b) F=1

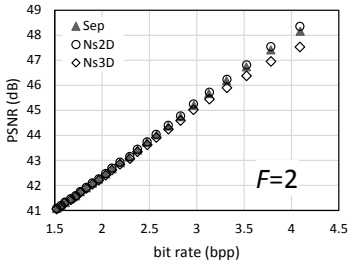

(c) F=2

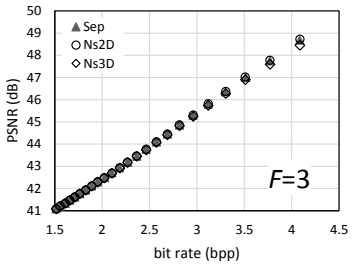

(d) F=3

Fig.12 Performance in lossy coding mode.

Another respect is relation between the bit depth F and the standard deviation of the rounding noise σ_{Rnd}. It is modelled as

$$\sigma_{Rnd}^2 \propto 2^{-F}. \qquad (31)$$

Therefore the upper bound increases as larger F is used. It is confirmed according to Fig. 12(b), (c) and (d). There is almost no difference among the existing method and the proposed method at F=3 as indicated in Fig. 12(d). It was observed that the proposed method is superior to the existing method in respect of PSNR at high bit rate in short length integer implementation of the transform.

Fig. 13 illustrates variance of the rounding noise in frequency domain. In this experiment, only one rounding operation in the forward transform is activated. The horizontal axis denotes # of the activated rounding operator which is numbered from up to bottom, from left to right in Fig. 4, 5 and 6. As summarized in Table I, Sep, Ns3D and Ns2D has 72, 24 and 40 rounding operations, respectively. It is noteworthy that total amount of the noise in Ns2D is increased even though the number of the rounding operation (= source of the noise) is increased from 24 to 40 comparing to Ns3D. The reason is considered to be relatively large variance (e.g. larger than 0.31) due to the rounding operation #8, #7, #6 and #5 in Ns3D. In contrast, all variances are less than 0.16 in Ns2D.

International Journal of Emerging Technology and Advanced Engineering
Website: www.ijetae.com (ISSN 2250-2459, ISO 9001:2008 Certified Journal, Volume 5, Issue 1, January 2015)

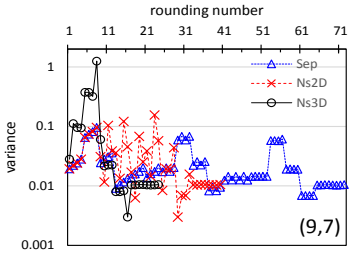

Fig.13 Effect of one rounding operation.

VI. Conclusion

In this paper, non-separable 2D structures were introduced instead of 3D structures in the existing method. Comparing to the existing method, total number of lifting steps was increased. However, total amount of rounding noise due to integer expression of signal values inside the transform (integer implementation) was decreased. It was confirmed that it contributes to increasing upper bound (quality of decoded images) in the rate distortion curve in lossy coding mode. Since tested input signals were limited to a few sets, more data sets should be tested in the future.

This work was supported by JSPS KAKENHI Grant Number 26289117.

REFERENCES

[1] Chao He, Dong, J., Zheng, Y. F., Zhigang Gao: Optimal 3-D coefficient tree structure for 3-D wavelet video coding, IEEE Trans. Circuits and Systems for Video Technology, vol.13, Issue 10, pp.961-972 (2003)

[2] B. Penna, T. Tillo, E. Magli, G. Olmo: Progressive 3-D coding of hyperspectral images based on JPEG 2000, IEEE Geoscience, Remote Sensing Letters, vol.3, issue 1, pp.125-129 (2006)

[3] Aggoun, A.: Compression of 3D integral images using 3D wavelet transform, IEEE Journal of Display Technology, vol.7, Issue 11, pp.586-592 (2011)

[4] Z. Xiong, X. Wu, S. Cheng, J. Hua: Lossy-to-lossless compression of medical volumetric data using three-dimensional integer wavelet transforms, IEEE Trans Medical Imaging, 22 (3), pp.459-70 (2003)

[5] Bing-Fei Wu, Chung-Fu Lin: A high-performance and memory-efficient pipeline architecture for the 5/3 and 9/7 discrete wavelet transform of JPEG 2000 codec, IEEE Trans. Circuits and Systems for Video Technology, vol.15, no.12, pp.1615-1628 (Dec. 2005)

[6] G. Shi, W. Liu, Li Zhang and Fu Li: An efficient folded architecture for lifting-based discrete wavelet transform, IEEE Trans. Circuits, Systems II express briefs, vol.56, no.4, pp.290-294 (April 2009)

[7] ISO / IEC FCD 15444-1, Joint Photographic Experts Group: JPEG 2000 image coding system, (March 2000)

[8] Skodras, A., Christopoulos, C., Ebrahimi, T.: The JPEG 2000 still image compression standard. IEEE Signal Processing Magazine, 18, pp.36-58 (2001)

[9] A. Descampe, F. Devaux, G. Rouvroy, J. D. Legat, J. J. Quisquater and B. Macq: A flexible hardware JPEG 2000 decoder for digital cinema, IEEE Trans. Circuits and Systems for Video Technology, vol. 16, issue 11, pp.1397-1410 (Nov. 2006)

[10] Kaneko, K., Ohta, N.: 4K applications beyond digital cinema. In: Proc. Int. Conf. Virtual Syst. Multimedia, pp. 133-136 (2010)

[11] M. Iwahashi, H.Kiya, Discrete wavelet transforms, InTech, ISBN 978-953-307-313-2, Chapter 14, Condition on Word Length of Signals and Coefficients for DC Lossless Property, pp.231-254, Sept. 2011.

[12] S. Chokchaitam, M. Iwahashi, Lossless / lossy image compression based on non-separable two- dimensional LWT", Proc. International Conference on Circuits / Systems Computers and Communications (ITC- CSCC 2002), pp. 912-915, (July 2002)

[13] S. Chokchaitam, M. Iwahashi, Lossless / lossy image compression based on non-separable two-dimensional L-SSKF, Proc. IEEE International Symposium on Circuits and Systems (ISCAS), pp.421-424 (May 2002)

[14] S. Fukuma, M. Iwahashi and N. Kambayashi: Adaptive multi-channel prediction for lossless scalable coding, IEEE International Symposium on Circuits and Systems (ISCAS), no.IV, pp. 467-470 (May 1999)

[15] M. Kaaniche, J. C. Pesquet, A. B. Benyahia, B. P. Popescu: Two-dimensional non separable adaptive lifting scheme for still and stereo image coding, IEEE International Conference on Acoustics, Speech, and Signal Processing (ICASSP), pp.1298-1301 (March 2010)

[16] M. Kaaniche, B. P. Popescu, A. B. Benyahia, J. C. Pesquet: Adaptive lifting scheme with sparse criteria for image coding, EURASIP Journal on Advances in Signal Processing: Special Issue on New Image and Video Representations Based on Sparsity, vol. 2012, pp.1-22 (Jan. 2012)

[17] M. Iwahashi, T. Orachon, H. Kiya: Three dimensional discrete wavelet transform with deduced number of lifting steps, IEEE International Conference on Image Processing (ICIP), no.WA.L4, pp.1651-1654 (Sept. 2013)

[18] M. Iwahashi, H. Kiya: Non separable 2D factorization of separable 2D DWT for lossless image coding, IEEE International Conference Image Processing (ICIP), pp.17-20 (Nov. 2009)

[19] M. Iwahashi, H. Kiya: A New lifting structure of non-separable 2D DWT with compatibility to JPEG 2000, IEEE International Conference on Acoustics, Speech, and Signal Processing (ICASSP), IVMSP, P9.7, pp.1306-1309 (March 2010)

[20] T. Yoshida, T. Suzuki, S. Kyochi, M. Ikehara: Two dimensional non-separable adaptive directional lifting structure of discrete wavelet transform, IEEE International Conference on Acoustics, Speech and Signal Processing (ICASSP), pp.1529-1532 (May 2011)

[21] T. Yoshida, T. Suzuki, S. Kyochi, M. Ikehara: Two dimensional non-separable adaptive directional lifting structure of discrete wavelet transform, IEICE Trans. Fundamentals, vol.E94-A, no.10, pp.1920-1927 (Oct. 2011)

[22] T. Strutz, I. Rennert, Two-dimensional integer wavelet transform with reduced influence of rounding operations, EURASIP Journal on Advances in Signal Processing, vol.2012, 2012:75, ISSN:1687-6180 (April 2012)

[23] M. Iwahashi, H. Kiya: Discrete wavelet transforms: Non separable two dimensional discrete wavelet transform for image signals, ISBN 980-953-307-580-3, InTech (2013)

[24] M. Iwahashi, T. Orachon, H. Kiya, Non separable 3D lifting structure compatible with separable quadruple lifting DWT, Asia-Pacific Signal and Information Processing Association 2013 Annual Summit and Conference (APSIPA), OS.26, IVM.11, no.4, pp.1-4 (Oct. 2013)